LEVEL II

12

AFWAL-TR-80-4152

53

# EXACT INVOLUTE BODIES OF REVOLUTION

N. J. Pagano

Mechanics & Surface Interactions Branch
Nonmetallic Materials Division



May 1981

Interim Report for Period June 1979 - June 1980

Approved for public release; distribution unlimited.



MATERIALS LABORATORY
AIR FORCE WRIGHT AERONAUTICAL LABORATORIES
AIR FORCE SYSTEMS COMMAND
WRIGHT-PATTERSON AIR FORCE BASE, OHIO 45433

E.U. 662

NOTICE

When Government drawings, specifications, or other data are used for any purpose other than in connection with a definitely related Government procurement operation, the United States Government thereby incurs no responsibility nor any obligation whatsoever; and the fact that the Government may have formulated, furnished, or in any way supplied the said drawings, specifications, or other data, is not to be regarded by implication or otherwise as in any manner licensing the holder or any other person or corporation, or conveying any rights or permission to manufacture, use, or sell any patented invention that may in any way be related thereto.

This report has been reviewed by the Office of Public Affairs (ASD/PA) and is releasable to the National Technical Information Service (NTIS). At NTIS, it will be available to the general public, including foreign nations.

This technical report has been reviewed and is approved for publication.

N. J. PAGANO, Project Engineer
Mechanics & Surface Interactions Br.
Nonmetallic Materials Division

S. W. TSAI, Chief
Mechanics & Surface Interactions Br.
Nonmetallic Materials Division

FOR THE COMMANDER

F. D. CHERRY, Chief
Nonmetallic Materials Division

"If your address has changed, if you wish to be removed from our mailing list, or if the addressee is no longer employed by your organization please notify AFWAL/MLBM, W-PAFB, Ohio 45433 to help us maintain a current mailing list.

Copies of this report should not be returned unless return is required by security considerations, contractual obligations, or notice on a specific document.

AIR FORCE/56780/27 November 1981 — 120

SECURITY CLASSIFICATION OF THIS PAGE *(When Data Entered)*

| REPORT DOCUMENTATION PAGE | | READ INSTRUCTIONS BEFORE COMPLETING FORM |
|---|---|---|
| 1. REPORT NUMBER<br>AFWAL-TR-80-4152 | 2. GOVT ACCESSION NO.<br>AD-A108 659 | 3. RECIPIENT'S CATALOG NUMBER |
| 4. TITLE *(and Subtitle)*<br>EXACT INVOLUTE BODIES OF REVOLUTION | | 5. TYPE OF REPORT & PERIOD COVERED<br>Interim Report<br>Period June 79 - June 80 |
| | | 6. PERFORMING ORG. REPORT NUMBER |
| 7. AUTHOR(s)<br>N. J. Pagano | | 8. CONTRACT OR GRANT NUMBER(s)<br>Inhouse Report |
| 9. PERFORMING ORGANIZATION NAME AND ADDRESS<br>Materials Laboratory<br>AF Wright Aeronautical Laboratories<br>AF Systems Command<br>Wright-Patterson AFB, OH 45433 | | 10. PROGRAM ELEMENT, PROJECT, TASK AREA & WORK UNIT NUMBERS |
| 11. CONTROLLING OFFICE NAME AND ADDRESS<br>Materials Laboratory, AFWAL<br>AF Systems Command<br>Wright-Patterson AFB, OH 45433 | | 12. REPORT DATE<br>May 1981<br>13. NUMBER OF PAGES<br>46 |
| 14. MONITORING AGENCY NAME & ADDRESS(*if different from Controlling Office*) | | 15. SECURITY CLASS. (*of this report*)<br>Unclassified<br>15a. DECLASSIFICATION/DOWNGRADING SCHEDULE |

16. DISTRIBUTION STATEMENT *(of this Report)*

Approved for public release; distribution unlimited.

17. DISTRIBUTION STATEMENT *(of the abstract entered in Block 20, if different from Report)*

18. SUPPLEMENTARY NOTES

19. KEY WORDS *(Continue on reverse side if necessary and identify by block number)*

Exact involute surface
Exit cones
Carbon-carbon exit cones
Rosette bodies
Rocket nozzles

20. ABSTRACT *(Continue on reverse side if necessary and identify by block number)*

Involute construction is an approach used in contemporary rocket nozzle technology for the fabrication of exit cones and other bodies of revolution and consists of laminating identical composite sheets of u;niform thickness along curved surfaces, called involute surfaces. In this work, we shall derive the exact solution for these surfaces, which guarantees that the volume of the body being generated is precisely filled, with no gaps or overlaps. We also present the equations of the developed surface, or ply

DD FORM 1 JAN 73 1473 EDITION OF 1 NOV 65 IS OBSOLETE

SECURITY CLASSIFICATION OF THIS PAGE *(When Data Entered)*

392 66 20

pattern, a formulation of the kinematics of the fabrication debulking process, and an experimental validation of the theoretical work.

## FOREWORD

In this report, the analysis leading to an exact method to construct bodies of revolution from thin sheet material is derived. Experimental validation and applications in the rocket nozzle industry are presented.

This report was prepared in the Mechanics and Surface Interactions Branch (AFWAL/MLBM) Nonmetallic Materials Division of the Materials Laboratroy, AF Wright Aeronautical Laboratories, Wright-Patterson Air Force Base, Ohio. The work was performed under Project 2419, "Nonmetallic Structural Materials", Task No. 241903, "Composite Materials and Mechanics Technology". The time period covered by this effort was from June 1979 to June 1980. Dr. Nicholas J. Pagano was the Laboratory project engineer.

The author would like to express his sincere appreciation to Dr. L. E. Whitford for his considerable help in the numerical analysis associated with this work.

This report will also be published in the Journal of the Engineering Mechanics Division of the American Society of Civil Engineers.

TABLE OF CONTENTS

LIST OF ILLUSTRATIONS

## NOTATION

| | | |
|---|---|---|
| $r, \theta, z$ | = | cylindrical coordinates |
| $R_1(z), R_2(z)$ | = | inner and outer radii, respectively, of body of revolution |
| $T$ | = | ply thickness |
| $c$ | = | involute constant |
| $N$ | = | number of plies |
| $\Phi$ | = | angle of rotation of EIS |
| $\alpha$ | = | arc angle |
| $\gamma$ | = | tilt angle |
| $\psi$ | = | surface angle |
| $\phi$ | = | helical angle |
| $\Omega$ | = | meridian angle in ply pattern |
| $\delta$ | = | helical convolute angle |
| $A$ | = | constant defined by Eq. (40) |
| $c_c$ | = | cylindrical involute constant |
| $w$ | = | helical arc length of helical convolute |
| $\ell$ | = | tangent length of helical convolute |
| $R_o$ | = | radius of cylinder in ply pattern |
| $\lambda$ | = | arc angle in ply pattern |
| $R, \textcircled{H}$ | = | plane polar coordinates in ply pattern |
| $z_p, z_{max}$ | = | minimum and maximum values of Z in EIS |
| $L$ | = | distance between reference points in ply pattern |
| $S$ | = | surface area of EIS |
| $s$ | = | arc length along involute |
| $V$ | = | volume of body of revolution |

| | | |
|---|---|---|
| $\hat{i}, \hat{j}, \hat{k}$ | = | unit vectors along $\theta$, r, z directions, respectively |
| $\hat{t}, \hat{s}, \hat{n}$ | = | unit vectors on EIS |

Overbars stand for parameters at arbitrary fixed point P on EIS.

Primes stand for undebulked parameters or $\theta'$ meridian.

# INTRODUCTION

Involute construction, formerly known as rosette construction, is a popular approach being used in rocket nozzle technology for the fabrication of exit cones and other bodies of revolution. Such bodies are formed by laminating identical fabric-reinforced composite plies of uniform thickness in such a way that each ply extends to the extremities of the body in both the radial and axial directions. Hence, the boundaries of the body are completely defined by the ply edges. The mathematical solution of this problem is the theme of this work.

The contemporary approach to involute construction incorporates the use of analysis and fabrication techniques that can lead to significant pre-existing flaw distributions within the body. Defects such as wrinkles and fabric distortion are induced and represent the suspected source of numerous failures that have occurred in test firings, and even in fabricated articles prior to imposed loadings. Regions of geometrical discontinuity, such as the neighborhood of a cylinder-cone intersection are particularly sensitive to the formation of this initial damage. The origin of many of these problems appears to lie in the use of an incorrect ply pattern, i.e., the basic ply geometry adopted does not satisfy the involute construction problem, which requires that a prescribed volume of revolution be filled precisely with a given number of identical plies of the same constant thickness.

The first analytical treatment of involute bodies appears to be due to Mamrol (Ref. 1) in an unpublished report. Other unpublished work was accomplished by workers at Hitco Corp. (Refs. 2,3). Pagano (Ref. 4) provided the first comprehensive treatment of cylindrical involute bodies, including the appropriate governing equations for the stress field in an elastic body under axisymmetric loading. Subsequently, an approximate method was presented (Ref. 5) to establish the ply pattern for bodies of conical shape. In the latter reference, it was assumed that one edge of the ply pattern is a straight line that coincides with the generator of a cone. It will be shown here that this assumption is only valid under very restrictive conditions. In most cases, the work in the study of involute bodies proceeds by first establishing the theoretical surface (called the involute surface) that satisfies the involute construction problem, following which an approach to develop that surface, i.e., the ply pattern generation scheme, is presented. The inverse problem of definition of the involute surface given a specific ply pattern was treated by Stanton and Pagano (Ref. 6), where an axisymmetric stress field model was also derived and used to examine the tendency of certain exit cones to delaminate under processing conditions. Since that treatment of the involute surface geometry was also approximate, the question of existence of a solution to the involute construction problem was naturally raised. In this work, we shall address this question.

In a parallel effort with the present work, E.E. Savage (Ref. 7) has postulated that a helical convolute surface satisfies the requirements of the involute construction problem. We shall provide the proof of this assertion in this presentation, as well as to rigorously derive the complete mathematical formulation that characterizes the aforementioned solution, including the equations that describe the ply pattern. An experimental demonstration of the present formulation shall also be given, as well as a model to characterize the kinematical response during the debulking process, which is an important part of the fabrication method.

## DEFINITION OF EXACT INVOLUTE SURFACE (EIS)

Consider a body of revolution generated by rotation of a plane region about the z-axis as shown in Figure 1. The boundary of the plane region is denoted by C, and conventional cylindrical coordinates $(r, \theta, z)$ will be employed in the formulation. Left- and right-hand segments of the contour C are introduced and defined by radial coordinates $r = R_1(z)$, $R_2(z)$, respectively. These two segments may either constitute the entire boundary C, as in Figure 1(a), or be separated at the upper and/or lower extremities by straight lines normal to the z-axis, such as the case illustrated in Figure 1(b). In general, the curve C must be represented by a piecewise-continuous function.

In practice, involute construction of bodies of revolution such as those shown in Figure 1* employs a lamination procedure utilizing identical plies of a constant thickness. This practice leads to the definition of the involute construction problem, which can be posed as a hypothetical problem that admits to a mathematically exact treatment, i.e., determine the equations of identical surfaces which are separated everywhere by a constant distance T measured in the local normal direction to the surface such that their boundaries completely define the surface of a given body of revolution (see Figure 2).

Hence, the volume defined by the boundaries of surfaces S is equivalent to the volume inside the body of revolution. If the body were actually formed from material layers or plies of thickness T whose boundaries follow the hypothetical surfaces S,

---

Figures are located in Appendix C

interior of the body would be filled such that no gaps occur between contiguous plies. A slight difference would exist between the material volume and the theoretical volume of the body of revolution because of the step-like appearance created by the plies at the boundaries. However, this difference vanishes as $T \to 0$ and does not exist at all in the hypothetical problem. The solution of the mathematical analog of the physical problem will be referred to here as the exact solution and the surface S will be called the exact involute surface (EIS).

## TRANSFORMATION RELATIONS

In this section, we shall formulate the approach which leads to the equation of the EIS. Our approach consists of examination of the relationship that exists between two surfaces, S and S', within the given body of revolution. The two surfaces are identical in size, shape, and all local geometric details, except that they are displaced from one another in the body. We shall discuss two successive transformations, which carry S into S', thence S' into S, such that the requirements of the mathematical analog are satisfied (see Figure 3).

In the first transformation, each point in S translates through the displacement $T\hat{n}$, where $\hat{n}$ is the local unit normal vector. This transformation maps S into S'.

The second transformation follows from the consideration of the geometry in the cylindrical involute problem (Ref. 4). In that case, we have shown that an annular region can be filled with identical curves, called involutes or spirals, which are

related to one another by rigid body rotations about the z-axis. Since each cross-section of our body of revolution is an annulus, this transformation is also appropriate in the present example. Hence, our second transformation, which carries S' back into S, consists of a rotation through an angle $\Phi$ about the z-axis, where $\Phi$ is a constant.

The two transformations above guarantee that the volume of a body of revolution can be filled with identical, uniformly spaced surfaces. As the surface S may extend indefinitely, we must truncate it at its intersection with the surface produced by revolution of curve C.

## MATHEMATICAL FORMULATION

Consider the trace of surface S that lies in the plane z = constant. It has been shown (Ref. 4) that a plane annulus can be filled by identical curves (involutes) related to each other by rigid body rotations about z. These curves are defined by the equation

$$r \sin \alpha = c \qquad (1)$$

where c is a constant and $\alpha$, called the arc angle, is the angle between tangents to the curve and the circle of radius r at the same point on the curve. In order to satisfy our second transformation, an equation of the form (1) must be satisfied within <u>each</u> cross-section of a general body of revolution. Thus, the general solution for the EIS takes the form

$$r \sin \alpha = c\,(z) \qquad (2)$$

where c is a function of z alone. It will now be necessary to review some of the basic relations needed to characterize surface geometry (Ref. 6).

Consider an infinitesimal element of a surface as shown in Figure 4. Two right-handed systems of unit vectors are shown in the figure: first, letting carets symbolize vector quantities, we have the orthogonal system $\hat{i}$, $\hat{j}$, $\hat{k}$, which lie in the positive $\theta$, r, and z coordinate directions, respectively; secondly, the non-orthogonal system $\hat{t}$, $\hat{s}$, $\hat{n}$. Here $\hat{t}$ is the vector tangent to the meridian $\theta$ = constant, $\hat{s}$ is tangent to the trace of the surface in the cross-section z = constant, and $\hat{n}$ is the normal vector pointing away from the interior of the body. Arc angle $\alpha$, tilt angle $\gamma$, and surface angle $\psi$ are also shown in Figure 4, where

$$\tan \gamma = \frac{dr}{dz} \tag{3}$$

$$\cos \psi = \hat{t} \cdot \hat{s} \tag{4}$$

and

$$\hat{s} = \hat{i} \cos \alpha - \hat{j} \sin \alpha \tag{5}$$

$$\hat{t} = \hat{j} \sin \gamma + \hat{k} \cos \gamma \tag{6}$$

Substitution of Eqs. (5) and (6) into (4) reveals the following interrelationship among the three angles

$$\cos \psi = -\sin \alpha \sin \gamma \tag{7}$$

and we shall restrict the ranges of the angles in this work according to

$$0 \leq \alpha \leq \pi/2, \quad 0 \leq \gamma \leq \pi/2, \quad \pi/2 \leq \psi \leq \pi \tag{8}$$

The unit vector $\hat{n}$ is given by

$$\hat{n} \sin \psi = \hat{t} \times \hat{s} \tag{9}$$

which, on use of Eqs. (5) and (6), becomes

$$\hat{n} \sin \psi = \hat{i} \sin \alpha \cos \gamma + \hat{j} \cos \alpha \cos \gamma - \hat{k} \cos \alpha \sin \gamma \tag{10}$$

We are now ready to invoke the first transformation of the preceeding section, i.e., local translation along $\hat{n}$.

We start from an arbitrary point p (r, $\theta$, z) that lies in surface S. From this point, we construct a normal vector $\Delta T\hat{n}$, which intersects S' at p' (r + $\Delta$r, $\theta$ + $\Delta\theta$, z + $\Delta$z) and is normal to S' at the latter point. Letting $\hat{R}'$ represent the position vector of p', we see that

$$\hat{R}' = r\hat{j} + \Delta T\hat{n} \tag{11}$$

Substitution of Eq. 10 into (11) leads to

$$(r + \Delta r)^2 \sin^2 \psi = r^2 \sin^2 \psi + (\Delta T)^2 \cos^2 \gamma + 2r\Delta T \sin \psi \cos \alpha \cos \gamma \tag{12}$$

along with

$$\sin \Delta\theta = \frac{\Delta T \sin \alpha \cos \gamma}{(r + \Delta r) \sin \psi} \tag{13}$$

and

$$\Delta z = \frac{-\Delta T \cos \alpha \sin \gamma}{\sin \psi} \tag{14}$$

We may now write an expression for $\hat{n}'$, the unit outward normal vector at p' in terms of $\alpha'$, $\gamma'$, and $\psi'$, and the basis vectors $\hat{i}'$, $\hat{j}'$, and $\hat{k}'$, where

$$\hat{i}' = \hat{i} \cos \Delta\theta - \hat{j} \sin \Delta\theta \tag{15}$$

$$\hat{j}' = \hat{i} \sin \Delta\theta + \hat{j} \cos \Delta\theta \tag{16}$$

Substituting Eqs. (15) and (16) into this expression and using the fact that $\hat{n}' \equiv \hat{n}$, we can show that

$$\alpha' - \alpha \equiv \Delta\alpha = -\Delta\theta \tag{17}$$

where $\alpha'$ is the arc angle at p'.

Let us next express Eq. (2) at point p', with

$$\Delta c = c(z + \Delta z) - c(z) \tag{18}$$

so that

$$(r + \Delta r)\ \sin\ (\alpha + \Delta\alpha) = c + \Delta c \tag{19}$$

Inserting Eq. (17), this becomes

$$(r + \Delta r)(\sin\alpha\ \cos\Delta\theta - \cos\alpha\sin\Delta\theta) = c + \Delta c \tag{20}$$

However, because of Eq. (13), we find that

$$\cos\ \Delta\theta\ =\ \frac{r\ \sin\ \psi\ +\ \Delta T\ \cos\ \gamma\ \cos\ \alpha}{(r\ +\ \Delta r)\ \sin\ \psi} \tag{21}$$

Finally, putting Eqs. (13) and (21) into (20) yields

$$r\ \sin\ \alpha = c + \Delta c \tag{22}$$

which, along with Eq. (2), implies that $\Delta c = 0$, or

$$r\ \sin\ \alpha = c = \text{constant} \tag{23}$$

Hence, the EIS must satisfy Eq. (23) in order to obey the first required transformation ($\Delta T\hat{n}$).

We shall now seek to establish the appropriate relations such that the second transformation (rigid body rotation) is satisfied. We first observe that Eq. (23) implies the following relation for a given value of z,

$$\theta(\alpha,z) - \overline{\theta}(z) = \overline{\alpha}(z) + \cot\ \overline{\alpha}(z) - \alpha(z) - \cot\ \alpha(z) \tag{24}$$

since Eq. (23) is the same equation that governs <u>cylindrical</u> involute geometry (Ref. 4). Here, $P(\overline{r}(z), \overline{\theta}(z), z)$ represents an arbitrary fixed point in S, while $\overline{\alpha}(z)$ is the arc angle at this point, and we have chosen to regard $\theta$ as a function of $\alpha$ and z in this relation. Of course, $\alpha$ and r are related everywhere via Eq. (23). For conceptual reas ns, one may choose the arbitrary fixed point to coincide with the intersection of the EIS at z

with the inner or outer surface of the body of revolution, i.e., $R_1(z)$ or $R_2(z)$ as shown in Figure 1, although this is not required.

In order to treat the rigid body rotation, it is necessary to consider the traces of two involute surfaces, S and S', cut by a plane z = constant since these traces map into each other in such a transformation. As before, we begin by constructing a vector $\Delta T\hat{n}$ from point P such that the tip of the vector intersects S' at $P'(\bar{r}(z) + \Delta\bar{r}, \bar{\theta}(z) + \Delta\bar{\theta}, z + \Delta z)$. Using primes to denote functions in S' and taking Eq. (17) into account, Eq. (24) gives

$$\theta'(\alpha', z + \Delta z) - (\bar{\theta}(z) + \Delta\bar{\theta}) = \bar{\alpha}(z) - \Delta\bar{\theta} + \cot(\bar{\alpha}(z) - \Delta\bar{\theta}) - \alpha'(z + \Delta z) - \cot \alpha'(z + \Delta z) \tag{25}$$

Equation (24) with z replaced by $z + \Delta z$ and Eq. (25) are the equations of the traces of S and S', respectively, at the level $z + \Delta z$. The rigid body rotation is therefore expressed by

$$\theta'(\alpha, z + \Delta z) - \theta(\alpha, z + \Delta z) = \Delta\Phi \tag{26}$$

since points with the same $\alpha$ also have the same r. In Eq. (24), $\Delta\Phi$ is a constant to be evaluated later on. Carrying out Eq. (26), with the aid of (24) and (25), leads to

$$\Delta\Phi + \Delta\bar{\theta} = \bar{\alpha}(z) + \cot \bar{\alpha}(z) - \bar{\alpha}(z + \Delta z) - \cot \bar{\alpha}(z + \Delta z) - \frac{\Delta z \cot \bar{\gamma}(z)}{c \cos \bar{\alpha}(z)} \tag{27}$$

where Eqs. (13), (14), and (21) have been used, as well as elementary trigonometric formulas. Also, we have defined

$$\Delta\bar{\theta} = \bar{\theta}(z + \Delta z) - \bar{\theta}(z) \tag{28}$$

and $\bar{\gamma}(z)$ is the tilt angle $\gamma$ at P.

In order to solve Eq. (27) for $\Delta\bar{\theta}$, we only need to determine the constants $\Delta\Phi$ and $\bar{\gamma}(z)$ in terms of known parameters since $\bar{\alpha}(z)$ is known from Eq. (23) if $\bar{r}(z)$ is given, e.g., $R_1(z)$ or $R_2(z)$.

Considering the angle $\Delta\Phi$ first, we note that

$$\Delta\Phi = \frac{2\pi}{\Delta N} \tag{29}$$

where $\Delta N$ is the number of "layers" or exact involute surfaces corresponding to thickness $\Delta T$ required to fill the annular space. Hence, we get

$$\Delta N = \frac{NT}{\Delta T} \tag{30}$$

where N is the number of "layers" of thickness T. Therefore

$$\Delta\Phi = \frac{2\pi\Delta T}{NT} \tag{31}$$

which, by virtue of Eq. (14), becomes

$$\Delta\Phi = \frac{-2\pi\Delta z \sin\bar{\psi}(z)}{NT \cos\bar{\alpha}(z) \sin\bar{\gamma}(z)} \tag{32}$$

where $\bar{\psi}(z)$ is the surface angle $\psi$ at P.

To define the tilt angle $\bar{\gamma}(z)$, we consider the meridian of the involute surface S containing point P. Let this meridian intersect the $z + \Delta z$ trace of S at $r = r_p$ ($\alpha = \alpha_p$). Thus, an approximate expression for $\bar{\gamma}(z)$ is given by

$$\tan\bar{\gamma}(z) \approx \frac{r_p - \bar{r}(z)}{\Delta z} \tag{33}$$

which becomes exact in the limit as $\Delta z \to 0$.

Writing Eq. (24) at $z + \Delta z$ and putting $\theta(\alpha_p, z + \Delta z) = \bar{\theta}(z)$ yields the result

$$\Delta\bar{\theta} = \alpha_p + \cot\alpha_p - \bar{\alpha}(z + \Delta z) - \cot\bar{\alpha}(z + \Delta z) \tag{34}$$

which brings Eq. (27) to

$$\Delta\Phi = \bar{\alpha}(z) + \cot \bar{\alpha}(z) - \alpha_p - \cot \alpha_p - \frac{\Delta z \cot \bar{\gamma}(z)}{c \cos \bar{\alpha}(z)} \tag{35}$$

Now using Eqs. (23) and (33) and elementary trigonometric identities, we can show that

$$\alpha_p = \bar{\alpha}(z) - \frac{\tan \bar{\gamma}(z) \tan \bar{\alpha}(z) \Delta z}{\bar{r}(z)} \tag{36}$$

in the limit as $\Delta z \to 0$, so that

$$\cot \alpha_p = \cot \bar{\alpha}(z) + \frac{\tan \bar{\gamma}(z) \Delta z}{c \cos \bar{\alpha}(z)} \tag{37}$$

Finally, substituting Eqs. (32), (36), and (37) into (35) while passing to the limit $\Delta z \to 0$, we find that

$$\frac{2\pi \sin \bar{\psi}(z)}{NT \cos \bar{\alpha}(z) \sin \bar{\gamma}(z)} = \frac{\tan \bar{\gamma}(z)}{c \cos \bar{\alpha}(z)} + \frac{\cot \bar{\gamma}(z)}{c \cos \bar{\alpha}(z)} - \frac{\tan \bar{\alpha}(z) \tan \bar{\gamma}(z)}{\bar{r}(z)} \tag{38}$$

which, after some elementary manipulations and the use of Eq. (7), yields

$$\tan \bar{\gamma}(z) = \frac{A}{\cos \bar{\alpha}(z)} \tag{39}$$

where

$$A = \frac{1}{NT} (4\pi^2 c^2 - N^2 T^2)^{\frac{1}{2}} \tag{40}$$

which is a constant. Clearly, we have

$$c \geq \frac{NT}{2\pi} \tag{41}$$

which controls the minimum value of c that can be utilized.

Given the expressions (32) and (39), we may now return to Eq. (27) to determine $\Delta\bar{\theta}$. We now define

$$\Delta\bar{\alpha} = \bar{\alpha}(z + \Delta z) - \bar{\alpha}(z) \tag{42}$$

Introducing Eqs. (39), (42), and (32), in conjunction with (7), into (27) and letting $\Delta z \to 0$, we arrive at

$$d\bar{\theta} = \frac{A}{c}\, dz + \cot^2 \bar{\alpha}(z)\, d\bar{\alpha} \tag{43}$$

On integration over the range $(z_o, z)$, Eq. (43) gives

$$\bar{\theta}(z) - \bar{\theta}(z_o) = \frac{A}{c}(z - z_o) + \bar{\alpha}(z_o) + \cot \bar{\alpha}(z_o) - \bar{\alpha}(z) - \cot \bar{\alpha}(z) \tag{44}$$

and by substitution into Eq. (24), we get

$$\theta(\alpha,z) - \bar{\theta}(z_o) = \frac{A}{c}(z - z_o) + \bar{\alpha}(z_o) + \cot \bar{\alpha}(z_o) - \alpha(z) - \cot \alpha(z) \tag{45}$$

which, along with (23), represents the general equation of the EIS. The point corresponding to $\alpha = \bar{\alpha}(z_o)$, $\theta = \bar{\theta}(z_o) = \theta(\bar{\alpha}, z_o)$, $z = z_o$ simply represents an arbitrary point on the EIS. Also, since this point is arbitrary, Eq. (39) can be written as

$$\tan \gamma\ (\alpha, z) = \frac{A}{\cos \alpha(z)} \tag{46}$$

so that the relation (46) is valid <u>everywhere</u> on the EIS.

An important feature inherent in the present formulation is the clear statement of the "input" or prescribed parameters necessary to define the EIS. Any combination of parameters that serve to uniquely define the following constants and functions constitute a necessary and sufficient input data set,

$$c,\ N,\ T,\ R_1(z),\ R_2(z),\ \theta_o \tag{47}$$

where $\theta_o$, the $\theta$-coordinate of any point in $R_1(z)$, or $R_2(z)$, is only needed to define the angular position of the EIS, not its shape or size, and $R_1(z)$ and $R_2(z)$ need only be piece-wise continuous functions. While contemporary manufacturing procedures and the approximate treatment (Ref. 5) assume that a trace of the involute surface in a meridional plane coincides with the

generator of a cone, the input parameters (47), which define the EIS, prohibit this assumption, in general. However, if we invoke the small $\alpha$ assumption $\alpha^2 << \alpha$, we find that Eq. (44) is satisfied by the conical trace $\bar{r}(z) = Kz$ <u>provided that A = K</u>, where A is given by Eq. (40) and K is a constant. In this case then, the conical trace is a good approximation.

<u>Apparent</u> singularities occur in Eqs. (27), (32), (35), and (38) for the case $\bar{\gamma}(z) = 0$. These are removed by appealing to Eqs. (7) and (14), which give, for example

$$\lim_{\gamma \to 0} \left( \frac{\Delta z}{\sin \gamma} \right) = -\Delta T \cos \alpha \tag{48}$$

The situation $\bar{\gamma}(z) = 0$ arises only when the constant A vanishes. This leads to

$$c_c = \frac{NT}{2\pi} \tag{49}$$

and corresponds to a <u>cylindrical</u> EIS, which is the significance of subscript c in Eq. (49). The present equations now reduce identically to those given earlier (Ref. 4) for cylindrical involute surfaces. In this regard, it is important to note that the generation of a cylindrical body does not require that the involute surface be cylindrical. An example of this will be shown later here.

The surface given by Eqs. (45) and (23) represent the exact solution for the mathematical problem of filling space with identical, uniformly spaced surfaces. These equations represent a helical convolute surface (Ref. 8). In the next section, we shall examine some of the basic parameters of the helical convolute since they lead to an expedient approach to develop the surface, i.e., to construct the ply pattern.

## DEVELOPMENT OF EIS

We now proceed to demonstrate that the EIS is a helical convolute of a cylinder of radius c. To start, we shall review the geometrical construction of the helical convolute (Ref. 8), which will be helpful in establishing the equation of the developed surface, or ply pattern.

The helical convolute is generated by a straight line which moves in space such that it remains tangent to a helix. The case where the end point of the line moves in a plane normal to the axis of the cylinder, which is important in the construction of involute exit cones; is depicted in Figure 5. In this figure, the helix on the cylinder of radius c is shown as OQT. The helical convolute is generated by PQO such that the sum of the helical arc length w = OQ and the tangent length $\ell$ = QP remains constant. In other words, the helical convolute is generated by wrapping a right triangular sheet of height OS and hypotenuse PQO on the cylinder. As a result of this geometrical construction, we can show that the coordinates of points P and Q are related by

$$\begin{aligned} r^2 &= (z - z_Q)^2 \tan^2\delta + c^2 \\ \sin(\pi/2 - \theta + \theta_Q) &= c/r \end{aligned} \tag{50}$$

By direct substitution, one can demonstrate that the relations (50) identically satisfy the EIS equations (45) and (23), provided that

$$\tan\delta = A \tag{51}$$

Now the angle $\delta$ is defined by

$$\tan\delta = \frac{cd\theta}{dz} \tag{52}$$

If we let the helix OQT represent the intersection of the EIS and the cylinder of radius c, Eq. (45) gives

$$d\theta = \frac{A}{c}\, dz \tag{53}$$

Substituting Eq. (53) into (52) shows that Eq. (51) is satisfied. Hence, the postulate that the EIS takes the form of a helical convolute (Ref. 7) has been proven. Finally, the tangent length $\ell$ is given by

$$\ell = (z - z_Q)\ \sqrt{1 + A^2} \tag{54}$$

In order to employ the more convenient base point O, it is only necessary to substitute the coordinates of point O in place of those for Q in the above relations.

Since the EIS is a helical convolute, it represents a single-curved, developable surface (Ref. 8). It follows that the helix of radius c is mapped into the arc of a circle of radius $R_o$, where

$$R_o = \frac{c}{\sin^2 \delta} \tag{55}$$

which, because of Eq. (51), becomes

$$R_o = c\ (1 + \tfrac{1}{A^2}) \tag{56}$$

Also, the lengths w and $\ell$ (Figure 5) are preserved in the mapping so that the path of any point such as P (which is an involute of a circle of radius c) is carried into an involute of a circle of radius $R_o$. Reference to Figure 6 indicates that the mapped image of point P is described by polar coordinates R, Ⓗ , where

$$Ⓗ = \pi/2 + \cot \lambda_o - \lambda - \cot \lambda \tag{57}$$

$$R \sin \lambda = R_o \tag{58}$$

and

$$\tan \lambda_o = \frac{R_o}{(z - z_p)\sqrt{1 + A^2}} \tag{59}$$

Using the first of Eqs. (50), along with (51) and the relation that derives from the preservation of arc length w, namely

$$z_Q - z_p = \frac{R_o (\textcircled{H} + \lambda - \pi/2)}{\sqrt{1 + A^2}} \tag{60}$$

we find that Eq. (57) can be put into the form

$$\cot \lambda = \frac{\sqrt{1 + A^2}}{R_o} \left( \frac{\sqrt{r^2 - c^2}}{A} - z + z_p \right) + \cot \lambda_o \tag{61}$$

and finally, using Eqs. (59) and (56), we get

$$\cot \lambda = \frac{A}{c} \sqrt{\frac{r^2 - c^2}{1 + A^2}} \tag{62}$$

which can also be expressed as

$$\cot \lambda = \frac{A}{\sqrt{1 + A^2}} \cot \alpha \tag{63}$$

Hence, once the EIS has been defined, an arbitrary point (r, $\theta$, z) in space is mapped into (R, $\textcircled{H}$) in developed space by solving Eq. (62) for $\lambda$ and substituting into (57) and (58), after using (56) and (59) to compute $\lambda_o$ and $R_o$. It must be emphasized that we have implicitly assumed that $z - z_p \geq 0$ so that $z_p$ must be chosen as the <u>minimum</u> value of z. The value of $z_p$ corresponds to the point O in Figure 5 at which w = O and is easily found from the equations of the EIS by repeated use of the relation

$$z_p = z - \frac{\sqrt{r^2 - c^2}}{A} \tag{64}$$

Here r and z are the coordinates of any point on the EIS and Eq. (64) is used to search for the minimum value of $z_p$, which will always correspond to a point on the outer boundary of the body of revolution being generated. Finally, since the EIS is a developable surface, we shall dispense with the distinction between the mathematical and physical solutions of the involute construction problem; they only differ because of the finite compliance of the sheet material and the "steps" on the boundary of the body constructed of sheets of constant thickness, as discussed earlier.

## ILLUSTRATIVE EXAMPLE

As an example of the use of the present model, the body of revolution having the profile shown in Figure 7 was built by involute construction. The geometry of this body is similar to that of contemporary rocket nozzle exit cone structures. The ply material used in the construction was heavy paper having a constant thickness of 0.01 in. Using this value for T, with $c = 0.15$ and $N = 92$, which satisfy the inequality of Eq. (41), the ply pattern generated via the present model, Eqs. (56)-(59), (62), and (64), is shown in Figure 8. The mapped positions of several involute trajectories ($z$ = constant) and meridians ($\theta$ = constant), which approximate straight lines for reasonably small values of $\alpha$, are also shown in the figure. The range of $\gamma$ in this body is given by $12.56° \leq \gamma \leq 12.78°$.

Following the ply pattern generation, the body of revolution was constructed by laminating 92 plies such that their inner

boundaries rested on the surface of the male mandrel defined by radii $r = R_1(z)$. Pre-forming the plies is convenient, though not necessary. A pre-formed ply in the shape of the EIS and the male mandrel are shown in Figure 9, as well as the body itself. In practice, the plies would be bonded together, however, in the present case, they are held in place by supporting rings as shown in Figure 9. The existence of this body, in accordance with the geometry prescribed in Figure 7, serves as an experimental demonstration of the validity of the present mathematical model. The body shown in Figure 9 could not be built using contemporary practice since the heavy paper material has no mechanism to produce the severe distortions associated with that practice. Thus the potential to build relatively defect-free structure is another virtue of the new approach.

There exists a sensitive dependence between ply pattern design and number of plies. For example, ply patterns to construct the same body as in Figure 9 with the same values of c and T, but corresponding to N = 90 and 91 are shown in Figures 10 and 11, respectively. This relationship is also accompanied by marked variations in tilt angle $\gamma$. While minimal variation occurs within a given body, the average values of $\gamma$ for the cases N = 90, 91 are approximately 17.6°, 15.2°, respectively.

The equations that define the general solution for the EIS imply certain inequalities that must be satisfied by the EIS parameters to guarantee a geometrically admissible solution. For example, because of Eq. (23), the constant c must be equal

to or less than the smallest value of r in the body of revolution being generated. In development space, the angle (H) must be single-valued, so that Eqs. (60) and (58) require

$$z_{max} - z_p \leq \frac{2\pi c \sqrt{1 + A^2}}{A^2} \tag{65}$$

where $z_{max}$ is the largest value of z in the body of revolution. Furthermore, the parameters c, T, and N must satisfy Eq. (41). Finally, fabrication constraints, which can limit the maximum and/or minimum size of a body, and can impose restrictions on central angle $\theta$, must also be taken into account in the design of involute bodies.

We have remarked earlier that cylindrical bodies can be constructed via non-cylindrical involute surfaces. This has been illustrated in the forming of the cylindrical region of the body shown in Figure 9. Conversely, we can show that non-cylindrical bodies can be formed via cylindrical involute surfaces. This may be illustrated by invoking Eq. (49) to define c and generating the ply pattern corresponding to Figure 7 according to the present model. All of our equations remain valid, with (27), (32), (35), and (38) being subject to the interpretation discussed in connection with Eq. (48). For values of the parameters, N = 200 and T = .01, the ply pattern shown in Figure 12 is generated.

## DEBULKING KINEMATICS

In practice, involute bodies are fabricated from sheets of cloth-reinforced composite material. In its initial (as received) form, this preimpregnated cloth material is uncured and relatively

thick (approximately twice the final cured thickness). It is in this form that the material is cut into the ply pattern and laminated against specially designed tooling. Because of the large thickness in this form, the involute surface differs considerably from that existing in the final state, which has governed the ply pattern design. The system is then debulked under a slight temperature rise and the application of pressurization on either the inner or outer surface, with the opposite surface being controlled by tooling. Subsequent curing, carbonization, and/or graphitization establish the final dimensions of the billet.

Because of the above fabrication procedure, it is important to define the configuration of the involute surface corresponding to material in its initial, undebulked form. It is also necessary in the execution of the debulking phase to pressurize against tooling that controls the profile of either final surface, i.e., $R_1(z)$, or $R_2(z)$ in Figure 1. It is also desirable that the latter ply boundary remains in contact with the tooling throughout the process. Unfortunately, the edge of the ply pattern in the initial (undebulked) configuration cannot, in general, coincide with the same control surface as that in the final configuration. An exact solution for the initial configuration is possible if we abandon the control surface requirement. Thus, we simply formulate the inverse problem: given the ply pattern, N, and a new ply thickness, define the corresponding EIS. In this case, we assume that the ply pattern construction via the involute

method (Figure 6) remains unchanged while a new value of c is computed by use of Eqs. (56) and (40), i.e.,

$$\left(\frac{c'}{R_o}\right)^3 - \left(\frac{c'}{R_o}\right)^2 + \left(\frac{NT'}{2\pi R_o}\right)^2 = 0 \tag{66}$$

where primes denote undebulked parameters. Equations (59) and (62) are now solved with the aid of (56) to give the corresponding r, z coordinates,

$$z' - z'_p = \frac{\sqrt{c'R_o}}{A'} \cot \lambda_o \tag{67}$$

and

$$(r')^2 = c'R_o\cot^2\lambda + (c')^2 \tag{68}$$

while a single value of z' (say $z'_p$) can be prescribed arbitrarily.

While the approach outlined in the previous paragraph is exact, it is not suitable for modern involute exit cone manufacture. Therefore, we shall now consider an alternate method which permits the appropriate edge of the ply pattern to lie extremely close to the control surface over a significant region in the initial configuration provided the ply pattern boundary has no discontinuities in the region. In this approach, the two end points of the ply pattern boundary in the (smooth) region, which we shall call reference points, lie on the control surface. The approach proceeds as follows:

a. Determine the ply pattern corresponding to the final (cured) state in the usual manner and compute the distance L between the two reference points in the R Ⓗ plane. We let the initial position of the first point coincide with its final location, while the second point is merely constrained to lie on the control surface.

b. For the first approximation, let the initial r, $\theta$, z coordinates of the second point coincide with their final values. Using Eqs. (45) and (23), compute the value of the constant c' for the initial configuration.

c. Compute the initial mapped coordinates (R', Ⓗ') of the first reference point by use of Eqs. (56)-(59) and (62) directly. Determine the initial spatial (r, z) position of the second point by using the facts that it must lie on the control surface and its image is at distance L from that of the first point in the ply pattern. Now compute the (R', Ⓗ') coordinates of the second point. It should be noted that the Ⓗ' coordinate involves an arbitrary (non-essential) constant $z'_p$.

d. At this time, we have the mapped coordinates of each reference point in two coordinate systems, (R, Ⓗ) and (R', Ⓗ'). Since the two images of each reference point must coincide, we now establish the relationship between the two sets of coordinates.

e. By using the previously derived relationship, determine the (R', Ⓗ') coordinates of the ply pattern. Finally, apply the inverted form of Eqs. (56)-(59) and (62), along with (45) and (23), to define the spatial positions of points on the ply pattern boundary.

Adjustment of the constant c' can be accomplished to achieve a closer fit between the initial ply pattern boundary and the control surface, whereupon steps (a) through (e) are repeated. The above procedure involves only elementary geometric relations in addition to repetitious use of Eqs. (56)-(59), (62), (45), and (23). Hence, these equations are not shown here. Use of this

procedure (first approximation only) leads to the profile shown in Figure 13 for the ply pattern of Figure 8, where the profile is based upon a ply thickness of .02 in, while the reference points referred to in the approach are selected as the extremities of the inner conical surface. All points on the ply boundary do not contact this surface although the deviations are imperceptible at the scale of Figure 13.

## CONCLUDING REMARKS

The general problem of involute construction - formation of a body of revolution by laminating identical sheets of constant thickness - has been treated in detail. The two transformations that were applied - movement of each point of the solution surface a constant distance in the surface normal direction followed by a rigid body rotation of the surface - guarantee complete filling of the required volume with no gaps or overlapping regions. The exact involute surface (EIS) thus satisfies all requirements provided the profile of the body of revolution is piecewise-continuous. The question of the uniqueness of the particular pair of transformations that were applied to carry the EIS into itself has not been addressed. However, the solution that satisfies the particular transformations and input data (47), i.e., Eqs. (45) and (23), does represent a unique surface, and, of course, satisfies the problem requirements. Thus, the very important question of existence of a solution to the general problem of involute construction has been settled.

We have rigorously shown that the EIS assumes the geometric form of a helical convolute, which was evidently first postulated

in unpublished work by Savage (Ref. 7). The helical convolute is a surface of single curvature that is capable of development by standard methods of descriptive geometry (Ref. 8). The closed-form equations that describe this developed surface, called the ply pattern, have also been presented here. These are Eqs. (56)-(59), (62), and (64). Certain inequalities that must be satisfied by the EIS parameters, including Eqs. (41) and (65), have also been established.

The existence of a developable solution surface implies that a defect-free body is a potential product of this work. This is in sharp contrast to the severe fabric distortion and wrinkles observed (Ref. 9) in contemporary involute exit cones. Demonstration of this point and some validation of the mathematical formulation have been provided by the construction of the experimental model shown in Figure 9.

Finally, an approach to describe the kinematics of the debulking process has been established. By use of this model, one can approximate quite accurately the condition that a ply boundary remains in contact with a fabrication tooling surface, provided the ply boundary contains no discontinuity in the region. Another use of this model is to predict the displacement field as a function of instantaneous ply thickness in the debulking process.

## APPENDIX A
## VOLUME AND SURFACE AREA

Letting S represent the area of the EIS and referring to Figure 4, we observe that

$$dS = ds \frac{dz}{\cos \gamma} \sin \psi \tag{A-1}$$

where ds is the infinitesimal arc length of an involute in the plane z = constant. From Reference 4, ds is given by

$$ds = \frac{-dr}{\sin \alpha} \tag{A-2}$$

Hence, (A-1) becomes

$$dS = \frac{-\sin \psi \, dr \, dz}{\cos \gamma \sin \alpha} \tag{A-3}$$

Substitution of Eqs. (7), (23), and (46) and use of elementary trigonometry brings (A-3) to

$$dS = \frac{-c(1 + A^2)^{\frac{1}{2}} \cos\alpha \, d\alpha dz}{\sin^3 \alpha} \tag{A-4}$$

Integrating and substituting Eqs. (23) and (40) yields

$$S = \frac{\pi}{NT} \int [R_2^2(z) - R_1^2(z)] \, dz \tag{A-5}$$

where the nomenclature of Figure 1 has been used. Hence, the known result

$$V = NTS \tag{A-6}$$

is identically satisfied by the present formulation. Here, V stands for the volume of the body of revolution.

## APPENDIX B
## HELICAL ANGLE

An important parameter in the analysis of mechanical response of involute exit cones is the helical angle $\phi$ (Ref. 6), defined as the local angle between the warp fibers in a ply and the meridian. Referring to Figure 14, we have the relation

$$\phi = \textcircled{H}_w - \textcircled{H}_t \tag{B-1}$$

where $\textcircled{H}_w$ is the constant angle between the warp direction in the ply pattern and an arbitrary axis and $\textcircled{H}_t$ gives the orientation of the mapped meridian (denoted by t in Figure 14).

In Figure 14, the dashed line marked s represents the mapped position of the local vector $\hat{s}$. Observe that the angle $\psi$, given by Eq. (7), is preserved in the mapping. Hence, we see that

$$\textcircled{H}_t = \pi/2 - \psi + \lambda + \textcircled{H} \tag{B-2}$$

Hence by use of Eqs. (57) and (61)-(63), we arrive at

$$\textcircled{H}_t = \pi - \psi + \frac{A}{\sqrt{1 + A^2}} \left[\frac{A}{c}(z - z_p) - \cot\alpha\right] \tag{B-3}$$

which, along with (B-1), produces the desired result.

# APPENDIX C

# FIGURES

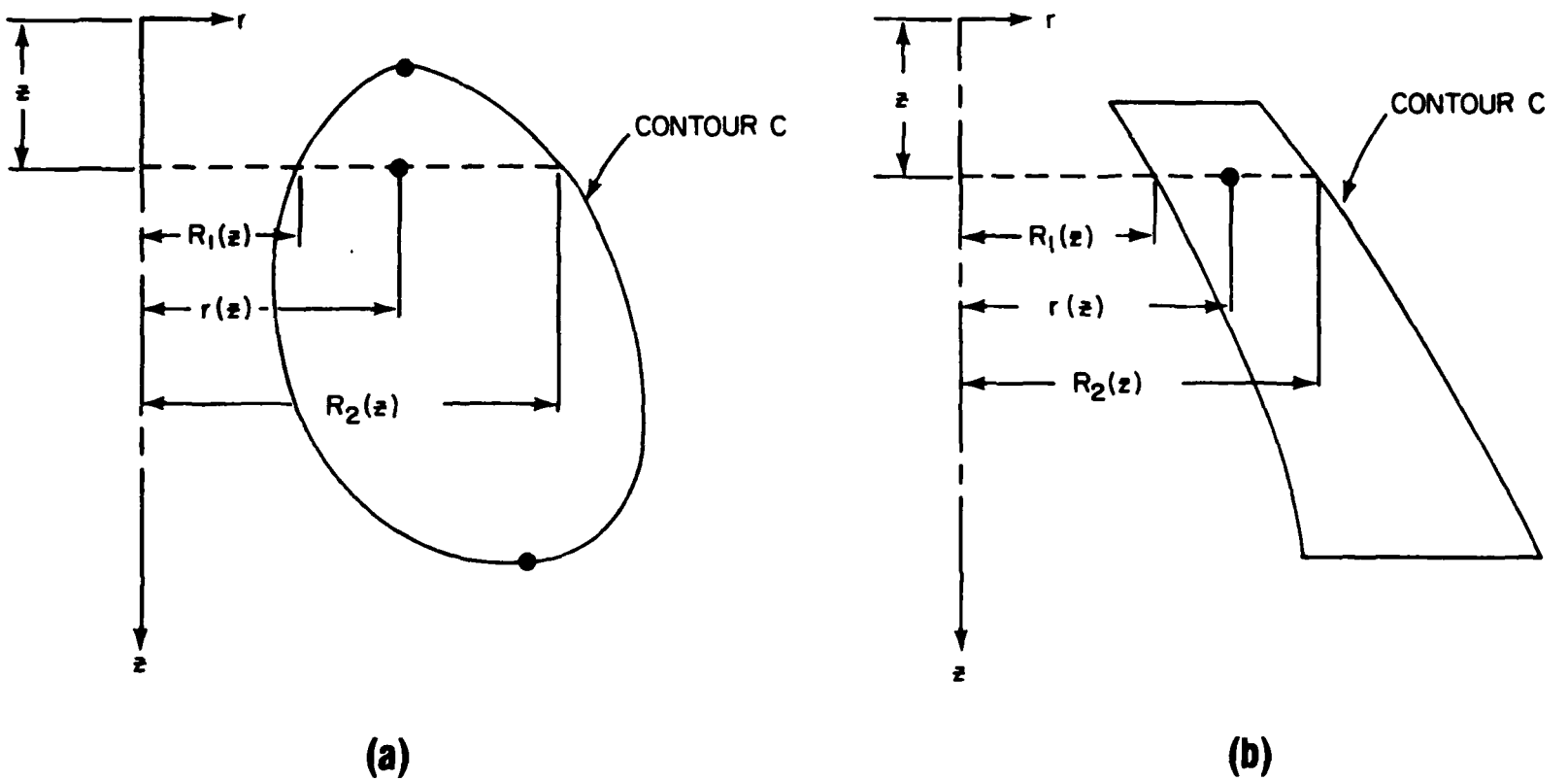


Figure 1. Bodies of Revolution

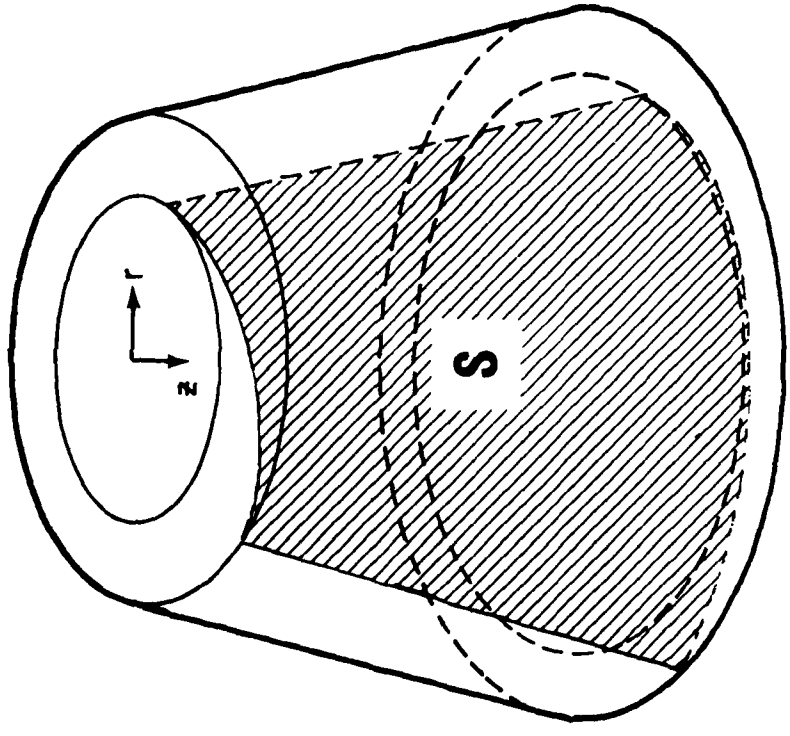


Figure 2. Exact Involute Surface of a Body of Revolution

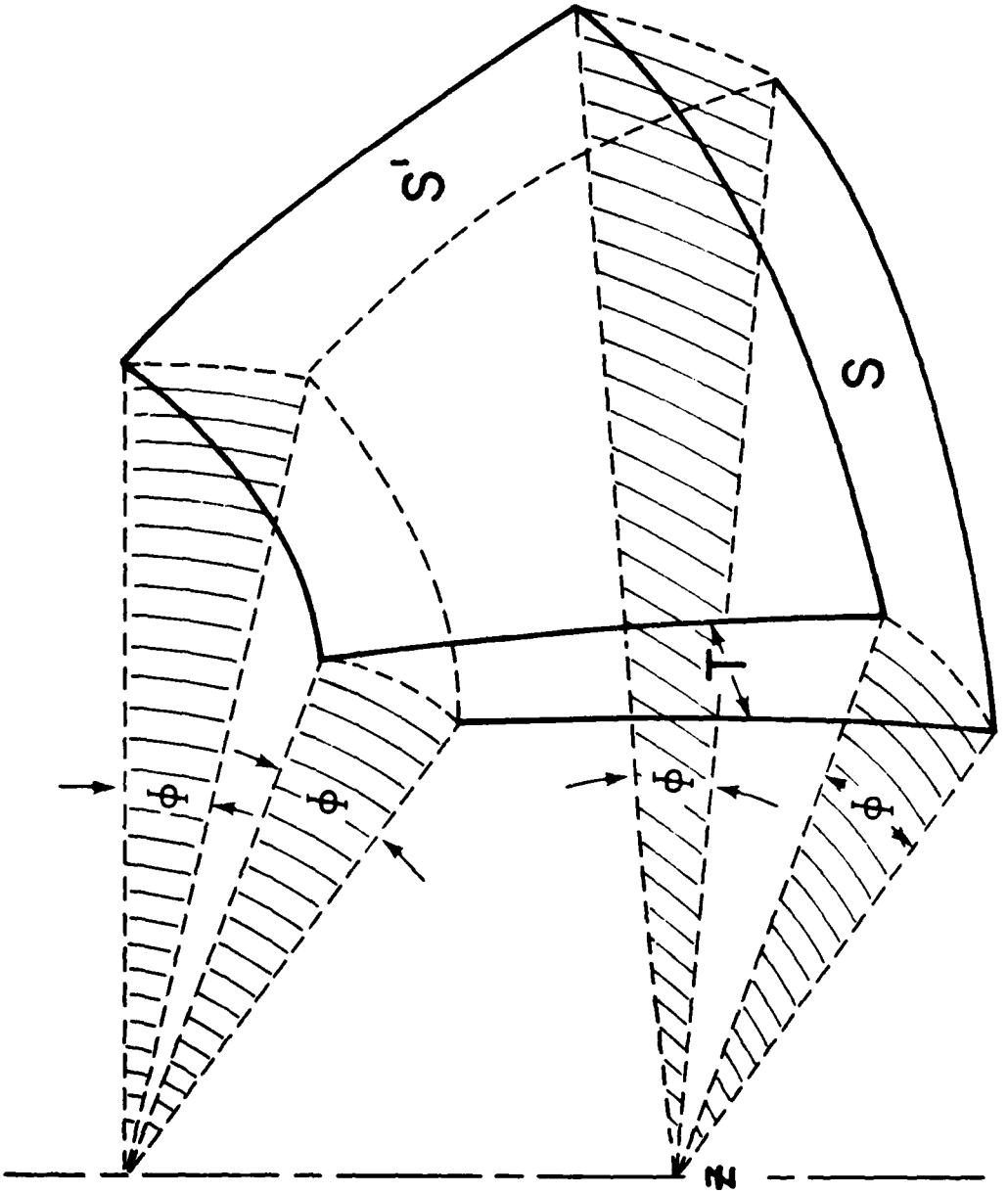


Figure 3. Surface Transformations

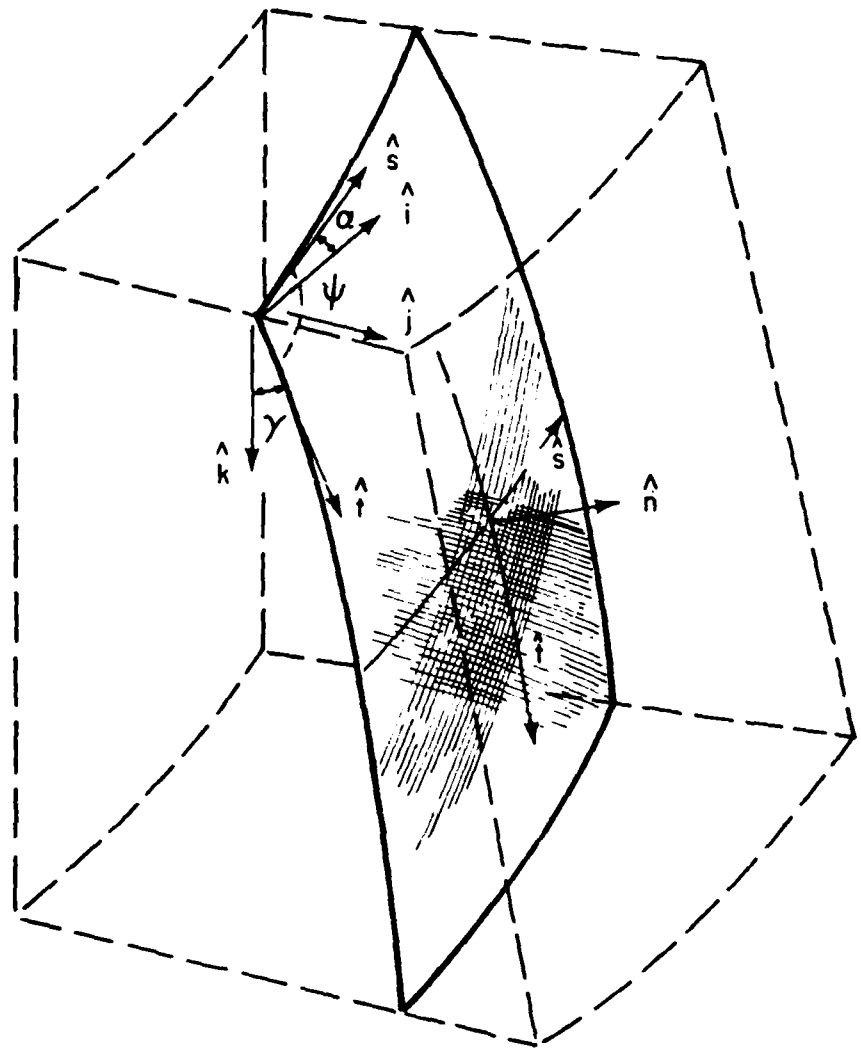


Figure 4. Basis Vectors for Involute Surface

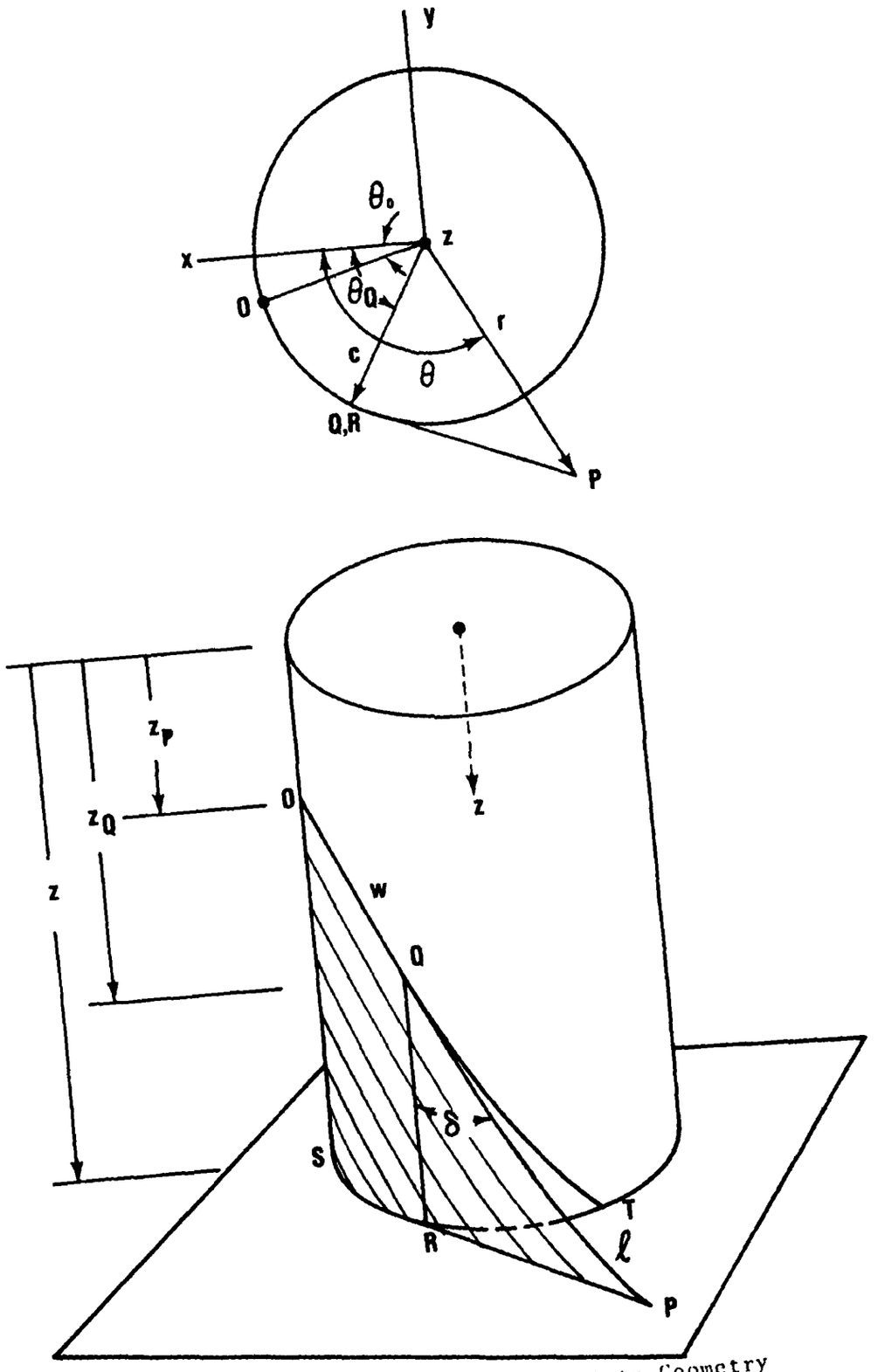


Figure 5. Helical Convolute Geometry

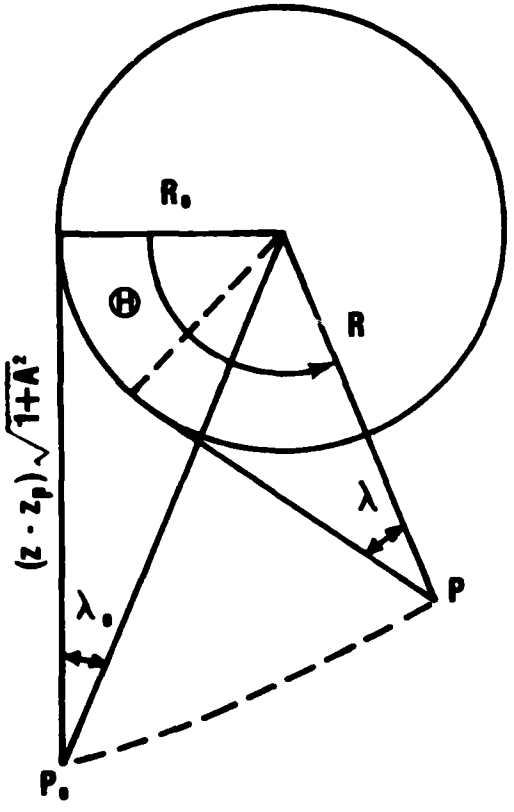


Figure 6. Development of Helical Convolute

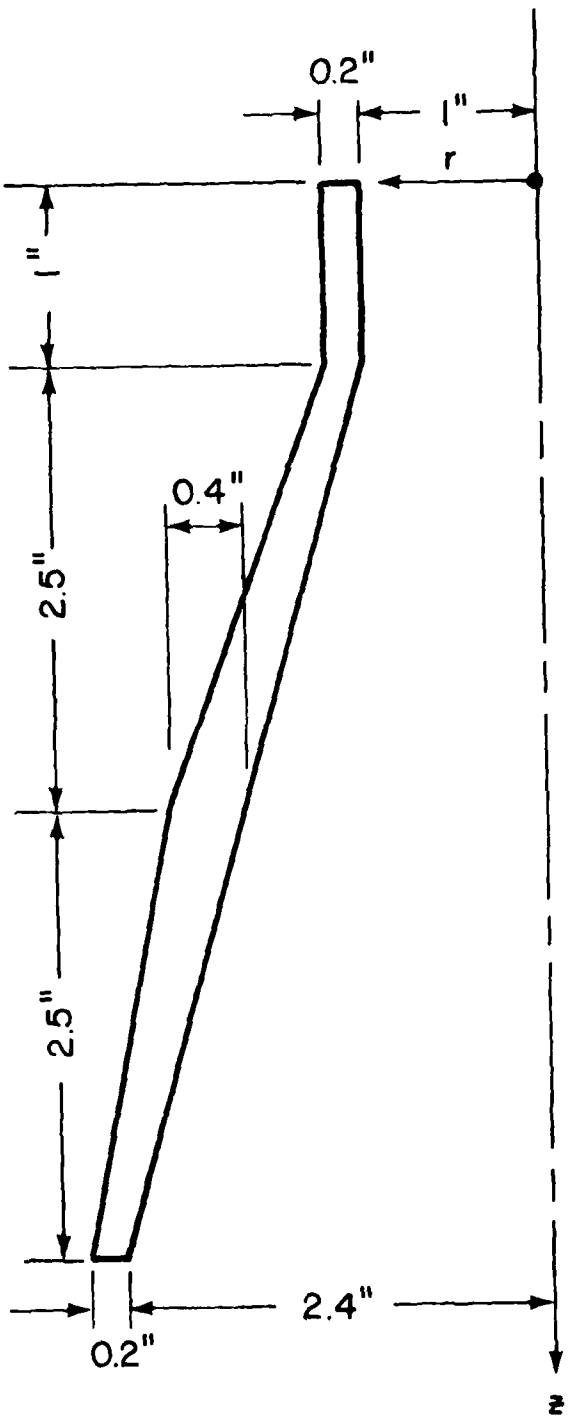


Figure 7. Exit Cone Model Profile

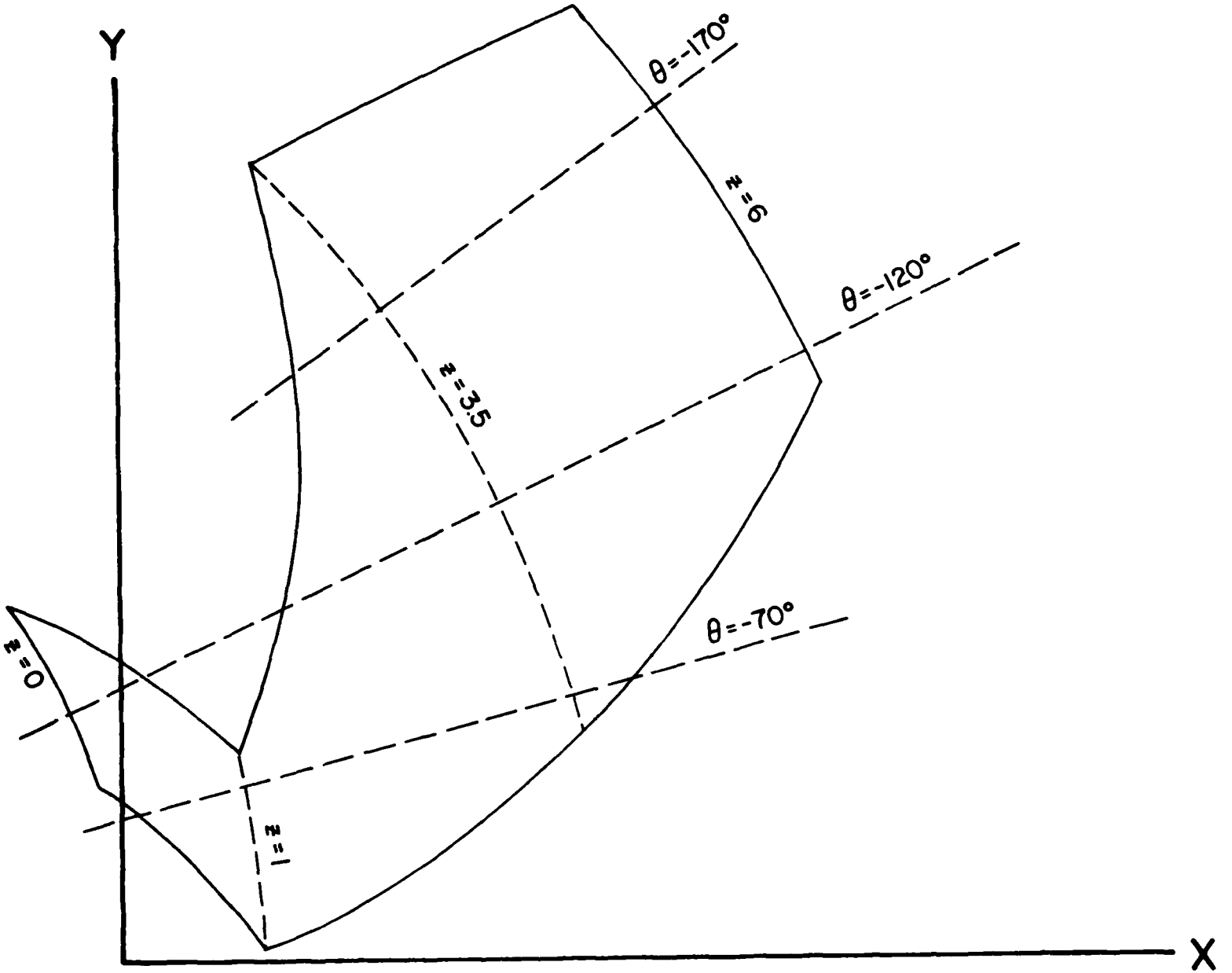


Figure 8. Ply Pattern for Exit Cone Model, N = 92

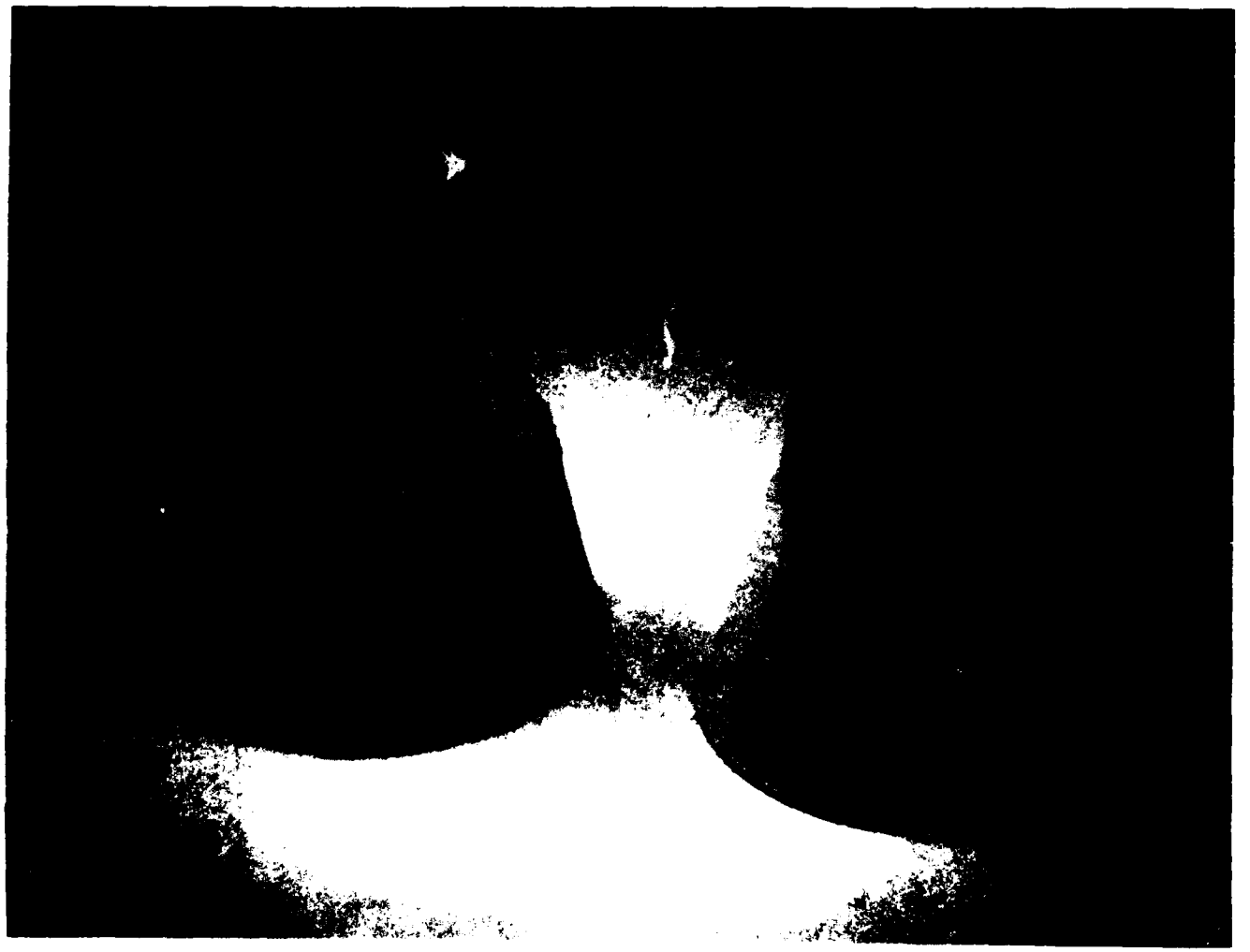

Figure 9. Exit Cone Model and EIS

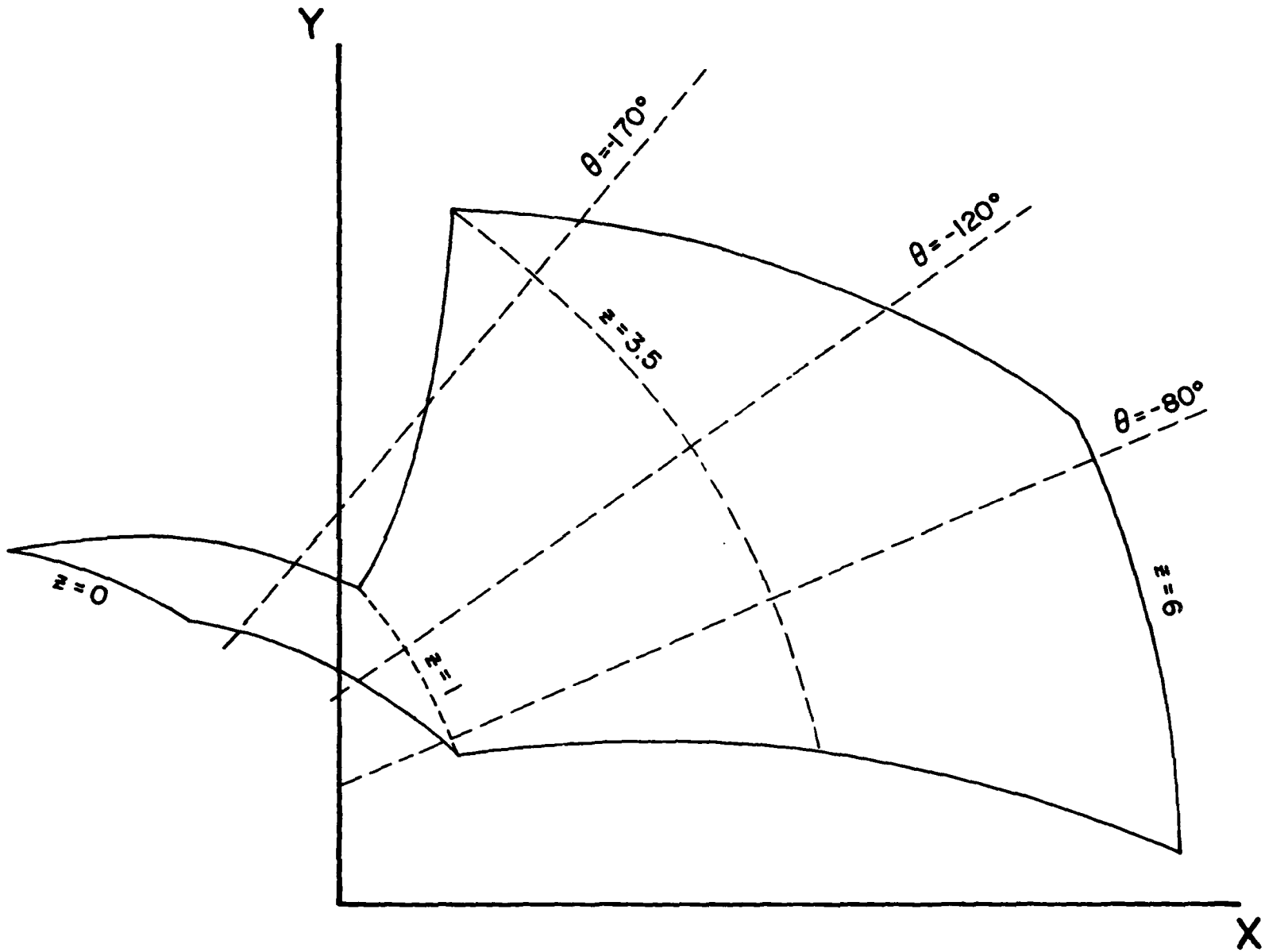


Figure 10, Ply Pattern for Exit Cone Model, N = 90

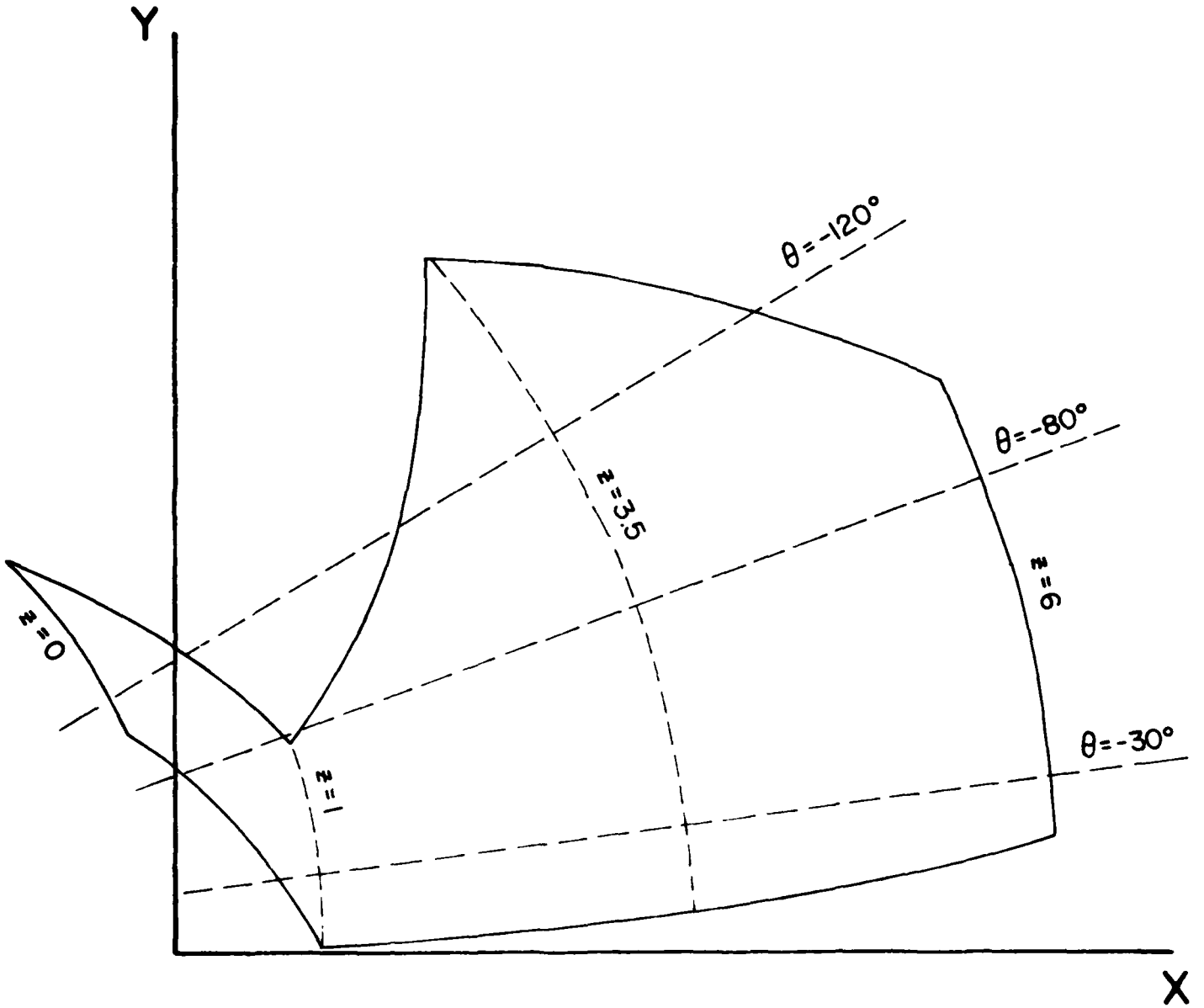


Figure 11. Ply Pattern for Exit Cone Model, N = 91

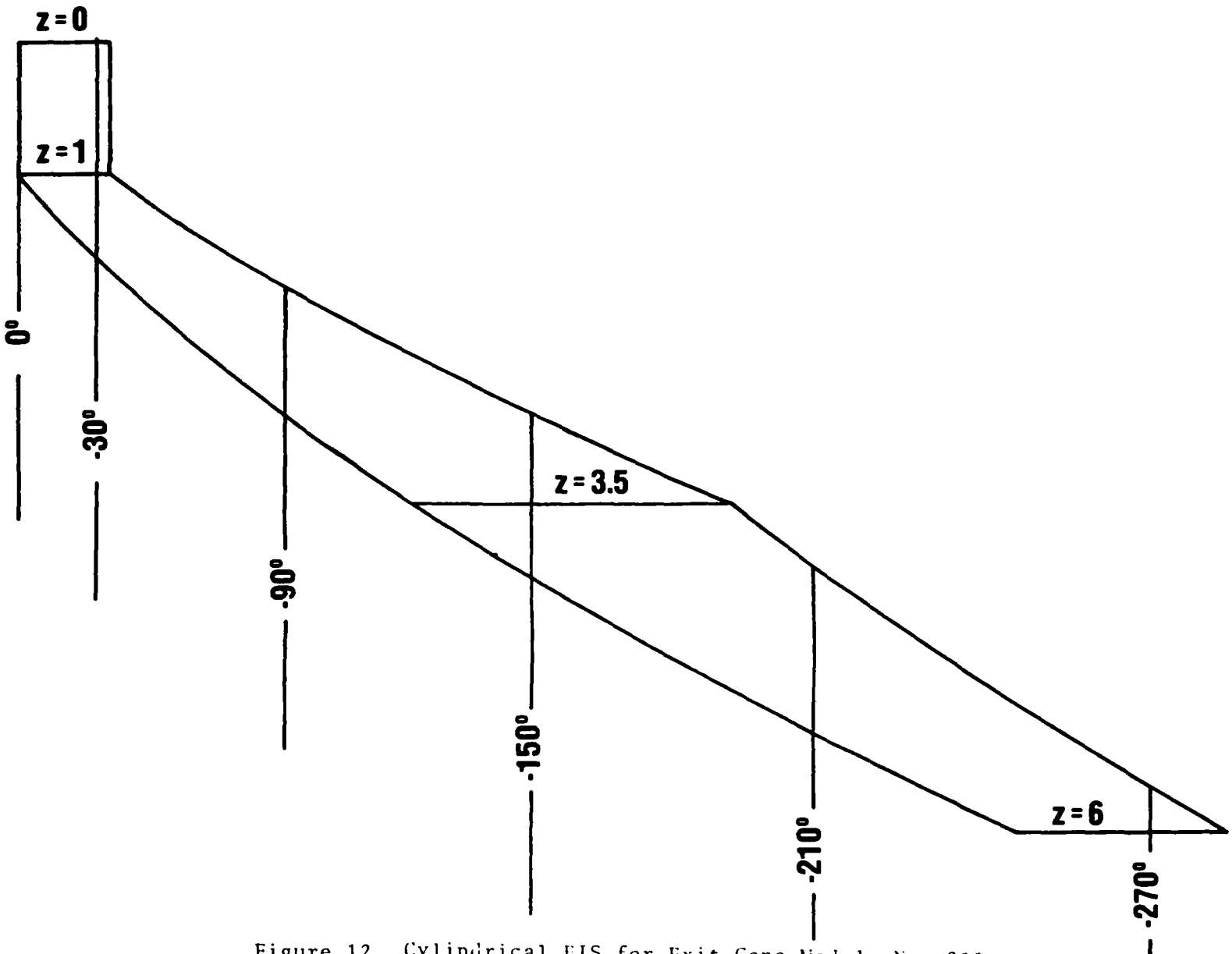


Figure 12. Cylindrical EIS for Exit Cone Model, N = 200

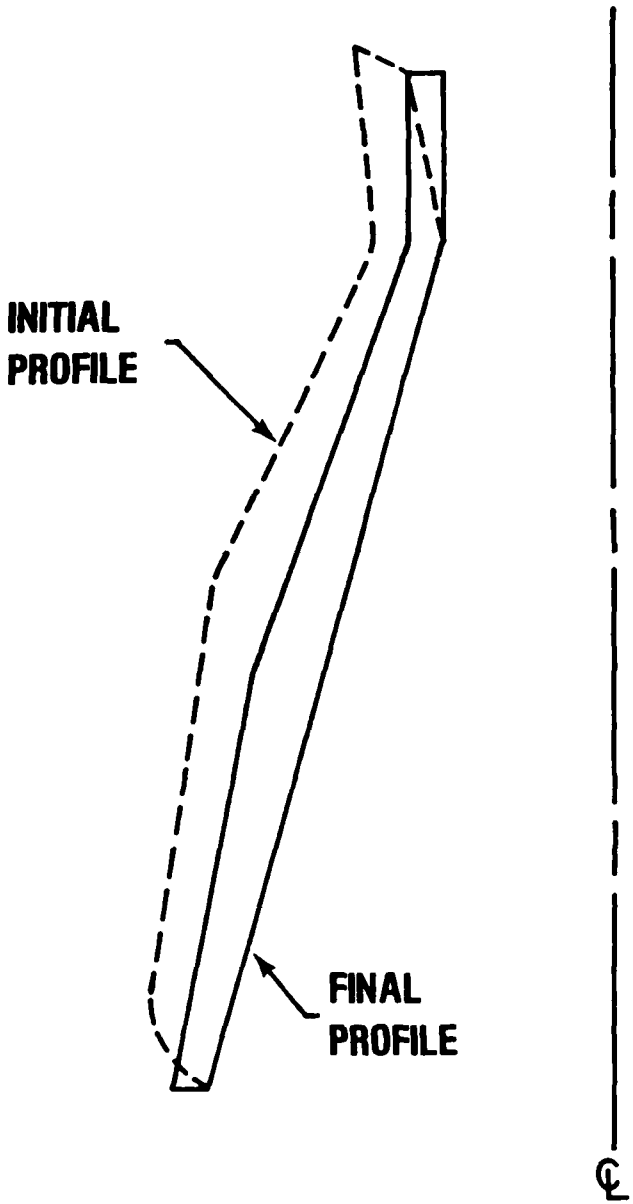


Figure 13. Model Lxit Cone Simulated Initial Profile, T = .02 in

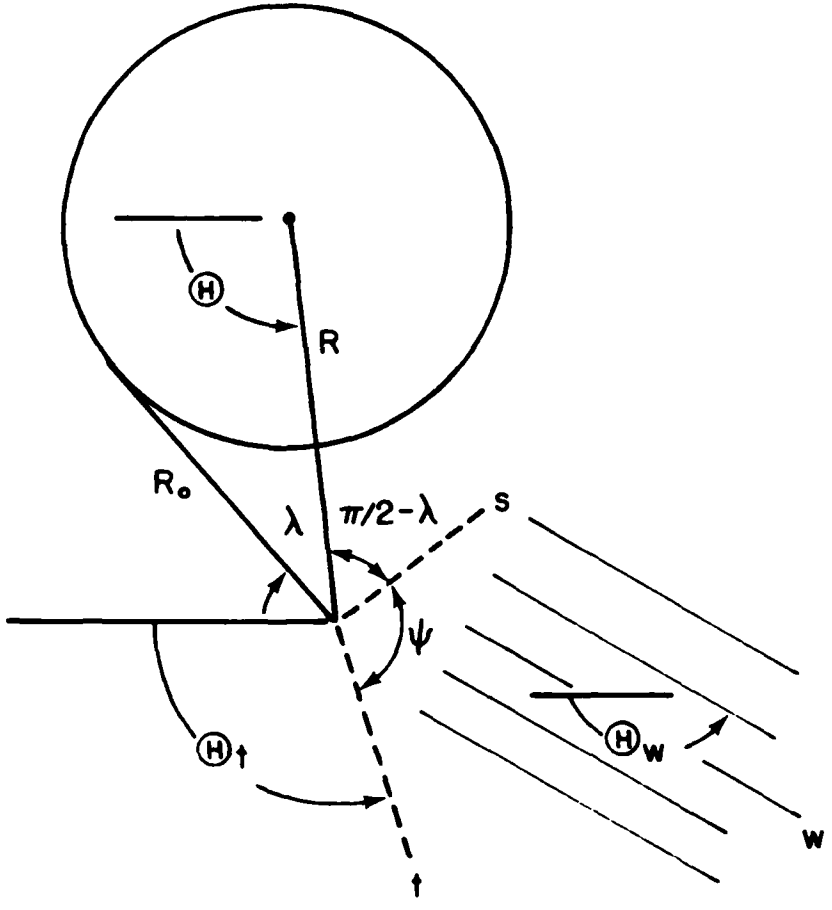


Figure 14. Ply Pattern Helical Angle

## REFERENCES


1. Mamrol, F. E., "Geometric Design Data - Rosette Lay-up," Rpt. 64SD262, General Electric, King of Prussia, PA, 1964.

2. Abildskou, D.P.A., "Rosette Analysis," Rpt. AD-66-1, HITCO Corp.

3. Zak, A., "Rosette Flat Pattern Analysis," Rpt. AD-66-4, HITCO Corp.

4. Pagano, N. J., "Elastic Response of Rosette Cylinders under Axisymmetric Loadings," AIAA Journal, Vol. 15, 1977, pp. 159-166.

5. Pagano, N.J. and Hsu, P.W., "Geometric Analysis of Rosette Exit Cones," Jour. Spacecraft and Rockets, Vol. 16, 1979, pp. 311-315.

6. Stanton, E.L. and Pagano, N.J., "Curing Stress Fields in Involute Exit Cones," Modern Developments in Composite Materials and Structures, J.R. Vinson, ed., The American Society of Mechanical Engineers, New York, 1979, pp. 189-214.

7. Savage, E.E., "The Geometry of Involute Construction," presented at the First JANNAF Carbon-Carbon Rocket Nozzle Technology Subcommittee Meeting held at Monterey, CA, 9-10 October 1979.

8. Wellman, B.L., Technical Descriptive Geometry, McGraw-Hill Book Company, Inc., New York, 1948.

9. Buch, J.D. and Pfeifer, W.H., "Process Stresses as Revealed by Microstructure and Microcracking," presented at the AFML Conference on Analysis and Fabrication of Carbon-Carbon Involute Exit Cones, Dayton, OH, 21-22 February 1979.




*U.S.Government Printing Office: 1981 — 559-006/5021